New Jersey Institute of Technology

Digital Commons @ NJIT

Summer 8-31-1998

Analysis of multi-lead QT dispersion by means of an algorithm implemented on Labview

Zafer Sahinoglu
New Jersey Institute of Technology

ABSTRACT

ANALYSIS OF MULTI-LEAD QT DISPERSION BY MEANS OF AN ALGORITHM IMPLEMENTED ON LABVIEW

by
Zafer Sahinoglu

QT dispersion measurement is significant in diagnostic ECG, and several methods are proposed in the literature to implement QT measurement.

This study consists of two parts: The first part was the development of an algorithm to measure both QT interval and QT dispersion. To check the reliability of the algorithm, 25 single channel ECGs were recorded and their QT intervals were computed. On two subjects, three and four lead ECG data were recorded respectively and their QT dispersions were statistically analyzed. Another part of this study dealt with the effect of the electric dipole of the heart on QT dispersion.

It was found that the mean and the standard deviation of the resulting QT dispersions were significantly smaller than those found in previous studies. In near and far field analysis, subjecting the data to a student's T test revealed that both near and far field QT dispersion data were drawn from the same population.

ANALYSIS OF MULTI-LEAD QT DISPERSION BY MEANS OF AN
ALGORITHM IMPLEMENTED ON LABVIEW

by
Zafer Sahinoglu

A Thesis
Submitted to the Faculty of
New Jersey Institute of Technology
in Partial Fulfillment of the Requirements for the Degree of
Master of Science in Biomedical Engineering

Biomedical Engineering Committee

January 1998

APPROVAL PAGE

ANALYSIS OF MULTI-LEAD QT DISPERSION BY MEANS OF AN ALGORITHM IMPLEMENTED ON LABVIEW

Zafer Sahinoglu

Dr. Stanley Reisman, Thesis Advisor   Date

Professor of Electrical and Computer Engineering, NJIT

Dr. Ronald Rockland, Thesis Advisor   Date

Assistant Professor of Electrical Engineering Technology, NJIT

Dr. David S. Kristol, Committee Member   Date

Professor of Chemistry, NJIT

BIOGRAPHICAL SKETCH

Author: Zafer Sahinoglu

Degree: Master of Science

Date: January, 1998

Undergraduate and Graduate Education:

- Master of Science in Biomedical Engineering,
  New Jersey Institute of Technology, Newark, NJ, 1998

- Bachelor of Science in Electrical Engineering,
  Gazi University, Ankara, Turkey, 1994

Major: Biomedical Engineering

To my beloved family

ACKNOWLEDGMENT

I would like to express my deepest appreciation to Dr. Stanley Reisman for his invaluable guidance, providing countless resources, insight and intuition. Also, special thank to Dr. Ronald Rockland for his encouragement, reassurance and literature support.

I would like to thank all my friends for putting up with me and providing good company. Especially, the help of Ahmet Candan with Microsoft Word processing as well as a being perfect roommate is beyond my description capability. Also, I thank Dr David Kristol for his taking place in my thesis committee.

TABLE OF CONTENTS

TABLE OF CONTENTS
(Continued)

Chapter   **Page**

LIST OF TABLES

LIST OF FIGURES

CHAPTER 1

INTRODUCTION

1.1 Objective

The objective of this study was to analyze multi-lead QT dispersion. To accomplish the objective, an algorithm was designed in Labview to compute QT dispersion derived from a multi-lead ECG signal. The algorithm was applied to the measurement of the dispersion in leads I, II, III (three limb leads). A study was then undertaken to compare the QT dispersion between near field and far field ECG measurement.

In past studies of QT dispersion, most of which used high speed paper analysis, only 2-3 consecutive beats were analyzed [5, 20]. Using a computerized system as in the present work, 2-3 minutes worth of multi channel ECG can be analyzed in terms of statistics developed on the average and standard deviation of the QT dispersion.

It was hypothesized that QT dispersion is influenced by the electric field caused by the heart dipole, and if the RA (right arm) and LA (left arm) electrodes were placed over the wrists and RL (right leg) and LL (left leg) electrodes over the ankles, the resulting QT dispersion of leads I, II and III would be expected to be smaller than if the electrodes were placed on the shoulders and below chest cavity. This would be due to the electric field of the heart dipole attenuating with an increasing distance from the dipole center.

1.2 Background Information

1.2.1 ECG

The electrocardiogram is primarily a tool for evaluating the electrical events within the heart. The action potentials of cardiac muscle cells can be viewed as batteries that cause charge to move throughout the body fluids. These moving charges, that is currents, represent the sum of the action potentials occurring simultaneously in many individual cells and can be detected by recording electrodes at the surface of the skin [16]. Figure 1.1
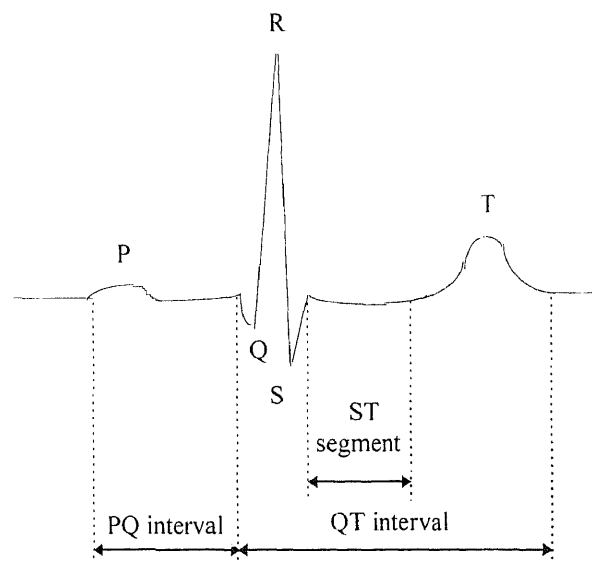
Figure 1.1 Lead II ECG signal.

illustrates a typical lead II ECG where the active electrodes are placed on the right arm and left leg.

The first deflection, the P wave, corresponds to current flow during atrial depolarization. Just before the P wave, the trace is flat, which means that the voltage

between the left leg and right arm is constant [16]. Normal P waves have various shapes,

from flat to sharply peaked with amplitudes ranging from 0 to 0.3 mv. The PQ interval,

extending from the beginning of the P wave to the first component of the QRS complex,

corresponds to the depolarization of the atria, AV node, AV bundle and its branches, and

the Purkinje system [16]. The PQ interval starts as depolarization begins in the atria and

stops when depolarization begins in the ventricles. The second deflection, the QRS

complex, is the result of ventricular depolarization. It is a complex deflection because the

paths taken by the wave of depolarization through the thick ventricular walls differ from

instant to instant and the currents generated in the body fluids change direction

accordingly [16]. The final deflection, the T wave, is the result of ventricular

repolarization. Atrial repolarization is usually not evident on the ECG because it occurs at

the same time as the QRS complex.

A typical clinical ECG makes use of 12 combinations of recording locations on

the limbs and chest so as to obtain as much information as possible concerning different

areas of the heart [18]. In practice, leads are taken in the *frontal plane* (the plane of the

body that is parallel to the ground when the subject is lying on his or her back) and the

transverse plane (the plane of the body that is parallel to the ground when the subject is

standing).

Three basic leads make up the frontal plane ECG (Figure 1.2) [18]. These are

derived when one electrode is located on the right arm (RA), the left arm (LA) and the

left leg (LL). A ground electrode is also placed on the right leg. The resulting three leads

are lead I (LA to RA), lead II (LL to RA) and lead III (LL to LA) [18]. The lead vectors

4

which are formed can be approximated as an equilateral triangle, known as Eindhoven's

RA_ I _+ LA

II III

LL
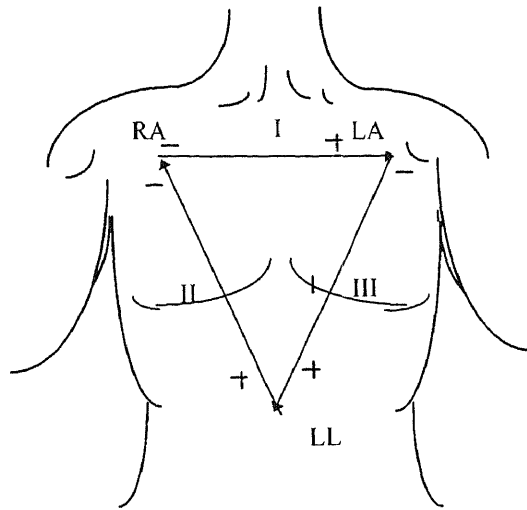
Figure 1.2 The Einthoven triangle and associated lead measurements [18].

triangle, in the frontal plane of the body as shown in Figure 1.2.

V_1 V_2 V_3 V_4 V_5 V_6
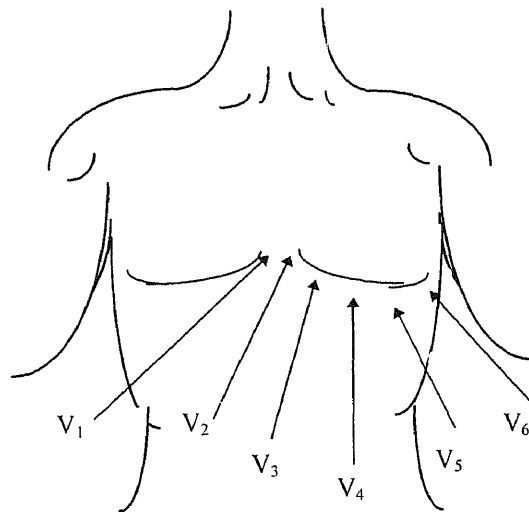
Figure 1.3 Positions of precordial leads (V_1 through V_6) on the chest wall [18].

When physicians look at the ECG in the transverse plane, they use six different precordial (chest) leads. They place the electrodes at various anatomically defined positions on the chest wall, as shown in Figure 1.3 [18].

Three additional leads are known as augmented leads, aVL, aVF and aVR [18]. Three limb electrodes are connected through equal valued resistors to a common node (Wilson central terminal). The augmented leads are obtained by removing the connection between the limb lead being measured and the central terminal.

It must be emphasized that the ECG provides information concerning only the electrical activity of the heart and the shapes and sizes of the P wave, QRS complex, and T wave vary with the electrode locations.

1.2.2 QT Interval and Dispersion

Measured from the beginning of the QRS complex to the end of the T wave, the QT interval relates to the duration of the depolarization and repolarization of the ventricles. It reflects regional differences in ventricular recovery time and may be a useful diagnostic tool to clarify myocardial infarctions [19]. Prolonged QT interval is an important electrocardiogram feature that currently is a subject of great interest as a clinical predictor of arrhythmia risk [5].

A single global QT interval measurement from the 12 lead electrocardiogram has been the standard measure, but recently there has been a great interest in the distribution

of the QT intervals, at a given instant of time, across the 12 lead electrocardiogram leads. This is called QT dispersion.

The QT dispersion is defined as the difference between the maximal and minimal QT interval duration among recorded leads at each specific beat [19]. The QT dispersion is believed to reflect local repolarization abnormalities and is emerging as an important new clinical tool. For instance, QT interlead variability (QT dispersion) has been shown to correlate better with the risk of arrhythmia than the QT interval itself. Increased dispersion of repolarization is known to be an important factor in the development of ventricular arrhythmias [22]. Also, according to research conducted in 1995, [5], an increased QT dispersion occurred in patients after myocardial infarction, in patients with long QT syndrome and in patients with hypertrophic cardiomyopathy. Moreover, the cardiovascular diseases associated with diabetes and uremia (ischaemic heart disease and left ventricular dysfunction) contributed to the increase in QT dispersion [22].

Furthermore, it has been revealed that patients with primary autonomic failure have prolongation of QT intervals, indicating that the autonomic nervous system is an important determinant of QT interval [27].

Considering all these results of previous studies, it can be said that QT dispersion analysis, possibly in combination with heart rate variability studies, should provide additional insight into the effects of left ventricular arrhythmias. In patients with long term diabetes, uremia, or both, computation of QT dispersion from the multi-lead ECGs may be a useful noninvasive method of estimating perioperative risk [22].

1.2.3 QT$_c$, Corrected QT Interval

The ability to define QT interval prolongation reliably is important because of its association with ventricular abnormalities [1]. However, identifying QT interval prolongation is hampered by the fact that the QT interval is not constant and highly dependent on the preceding cardiac cycles and therefore on heart rate [1]. QT interval varies not only with heart rate, but also with many other factors, including gender and, because of diurnal variability, time of day. Also, it has been shown that the autonomic nervous system may influence the QT interval independently of the heart rate [27]. To correct for this inconstancy, a rate-normalized or corrected QT interval QT$_c$ is used.

The object of the QTc is to normalize the QT interval to the value that it would have had if the heart rate were 60 beats/min, that is QT$_c$=QT when RR interval is equal to one second. One of the first, and still most widely used, QT correction formula was developed by Bazett [11]. In Bazett's formula QT$_c$ is defined as the QT interval divided by the square root of the current R to R time average ($QT_c = QT / \sqrt{RR}$) [1]. RR is the duration between the two consecutive R waves which occurs during ventricular depolarization. In the present study, as an average RR, the mean of the last three RR intervals was used to involve the effect of previous cardiac cycles. The QT correction formula was derived by defining the QT as the QTc when RR=1 sec, and solving for the resulting expression [1]. Because the Bazett's formula tends to be inaccurate at high and low ends of the range of heart rates, many other empirical formulas have been developed. However, there is no agreement as to which is the best method for QT correction, and

Bazett's formula remains the best known and most widely accepted method for rate normalization of QT interval.

1.2.4 Problems in QT Interval Algorithm

In the study of ventricular activity, it is important that the QT interval is measured correctly. Therefore, an algorithm to accurately detect QRS complex onset points and T wave end points is of great importance to compute QT intervals.

Several technical factors complicate the measurement of QT dispersion. The determination of the end of the T wave varies from study to study. The end of the T wave is often difficult to resolve as the return to the baseline of the slow moving deflection, often contaminated with noise, must be identified [21].
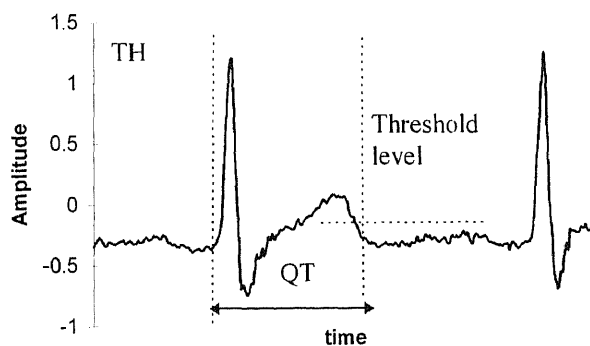
Figure 1.4 Illustration of the technique "threshold" to detect the end of the T wave [21].

Currently, the main algorithms for determining the end of the T wave include the interception of a threshold level and the T wave (TH), the interception of a threshold level

and the differential of the T wave (DTH), and the interception of a line characterizing the slope of the end of the T wave and the isoelectric level (SI) [21].

In the TH (threshold) technique, the magnitude of the detected T wave peak is multiplied by a coefficient to determine the threshold level, and then the threshold crossing point on the pure ECG signal is detected as the T wave end as shown in Figure 1.4.

Low Pass Filtered ECG
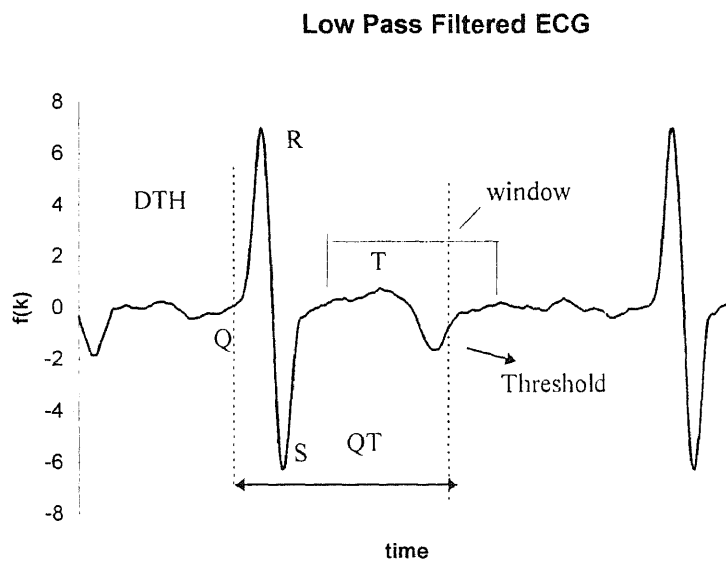
Figure 1.5 The illustration of the DTH "differential threshold method" to detect T wave end [21].

Figure 1.5 shows the differential threshold method (DTH) to detect T wave ends. In this method, a search window is defined to find the highest maximum or minimum point between the limits of the window which is located after the QRS complex. Then,

the amplitude of the maximum or minimum is used to determine the threshold value. Afterwards, the threshold crossing point is detected as illustrated in Figure 1.5.

Moreover, in the technique SI (slope intercept) the end of the T wave is identified as the intercept of an isoelectric level and a line tangential to the point of maximum T
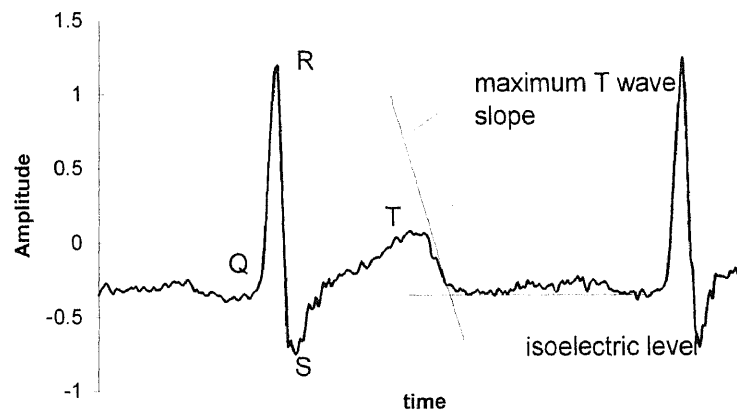
Figure 1.6 Illustration of the technique SI (slope intercept) to detect the T wave end [21].

wave slope. The SI technique is illustrated in Figure 1.6.

In this study, the DTH method was used for T wave end detection The variations applied to T wave end detection algorithms change depending on the type of differentiating filter used in the DTH method, the threshold, and isoelectric levels as well as the method of slope characterization.

1.3 Literature Review

Dispersion of repolarization, the difference in repolarization duration among several electrocardiographic leads, has been proposed as a measure of repolarization activity [26]. However, in the literature, the measured QT dispersion values vary among different studies in terms of the mean and the standard deviation. Previous papers studying QT dispersion involved reading of the ECG from paper sheets produced at high speeds. A 12 lead surface ECG at a paper speed of 50 mm/sec was recorded for healthy subjects and the resulting QT dispersion had the value of 38 ± 14 (mean $\pm$ SD) ms [5]. In another study in which a digitizer tablet was used to measure QT intervals, the average QT dispersion was 30 ± 10ms and QT_c dispersion 34 ± 11ms. Also, the maximum QT dispersion found was 53ms among 50 subjects [19]. Another study found the mean value of 19 ms for QT dispersion [6].

In the present study, the QT dispersion was smaller than the values mentioned above. The number of the leads used was just three. More than four channels were not able to be used because of the equipment problem. The ECG machine had three working channels out of four. Therefore, the possible effect on the QT dispersion by the precordial leads was not counted. These different results prove that the value of QT dispersion may vary, depending on which method is used.

The results obtained by means of manual and automatic measurement techniques may be different from each other. If a digitizer tablet is used, the resolution (the time between consecutive data points) is determined by the speed of the paper recording the

ECG signal. In a computerized process, it is set by the sampling frequency. For instance, if the sampling frequency is 100 Hz, the resolution, the time between adjacent samples, is 10ms. At this resolution, if the algorithm detects the (n-1)[th] sample instead of the nth sample, the resulting error would be 10 ms. In previous studies, the normal QT_c is often stated to be smaller than 440ms [4, 2]. However, strong evidence that the upper limit of normal QT_c is 440ms does not exist [3]. It was found that the normal QT_c ranged from 463ms to 506 ms [7], which is similar to the range of QT intervals (336 to 487 ms) reported in 50 normal subjects by Mirvis [10]. These findings were consistent with the value of QT intervals obtained in the present study.

There are some research results which support the idea that the three limb leads are influenced less by the heart dipole than the chest leads, leads V_1 through V_6. According to research done in 1994 [24], it is reported that in a population of patients with congenital long QT syndrome, assessment of QT dispersion in the 6 chest leads correlated well with the results obtained from analysis of all 12 ECG leads . It may be concluded that these 6 leads are mostly determining the QT dispersion value. Also another study [21] has revealed that the largest values for the standard deviation for all automatic QT measurement techniques occurred for lead V_1 which is one of the nearest points to the heart dipole. Moreover, it is shown in another research study that the longest QT interval is most frequently in leads V_1 through V_5 [22]. Based on all these findings, it appears that the further from the heart the limb lead electrodes are placed, the less affected they are by QT dispersion. In a later study, the observation of a 0.04 second difference in the QT duration among only 3 limb leads (I, II, III) were determined [25].

However, it is unclear whether dispersion parameters have independent predictive value from other ECG variables such as a dipole effect of the heart. This point needs highlighting and the study here may give an answer to that question.

1.4 The Concept of Electric Field

Faraday conceived of the space in the vicinity of electric charge as having different properties from ordinary space. It is characterized by a unique property that it is able to exert forces on charged particles within it, and it is called today *the electric field* [14].

The electric field in Faraday's model is associated with 'tubes of force' or 'lines of force' which are said to flow in the direction of the force exerted on a positive charge inserted in the field. This illustration is shown in Figure 1.7. These lines always originate (by convention) from a positive charge and terminate on a negative charge [14]. Charged bodies in the vicinity of uncharged ones have the lines of force asymmetrically arranged and terminated on charges of opposite sign induced on the nearest walls or masses.
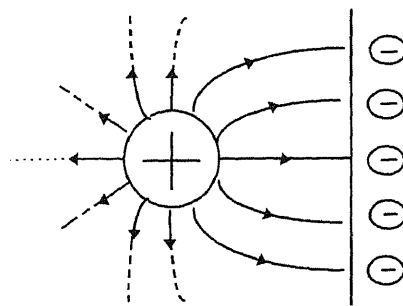
Figure 1.7 Example of non-symmetrical electric field [14].
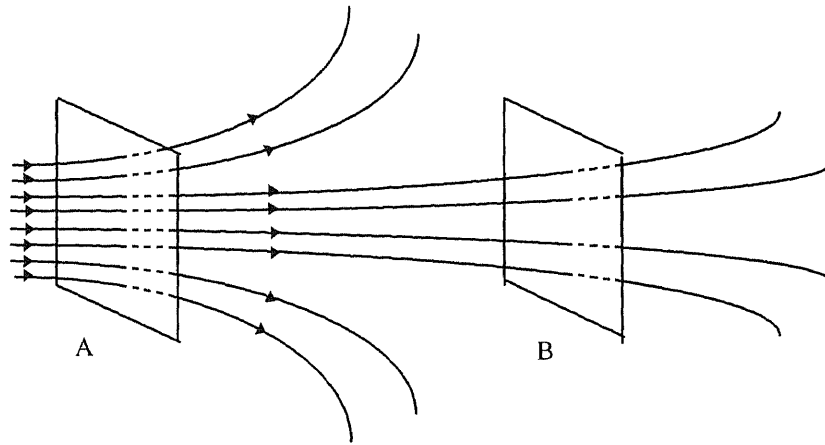
Figure 1.8 The field strength is proportional to the number of lines n threading through unit area A, or E=n/A [14].

To depict the field strength at various points, lines of force are drawn so that the density of the lines is proportional to the intensity. In Figure1.8, the field strength at point A is twice that at B because twice as many lines per unit area are counted through A compared to B.
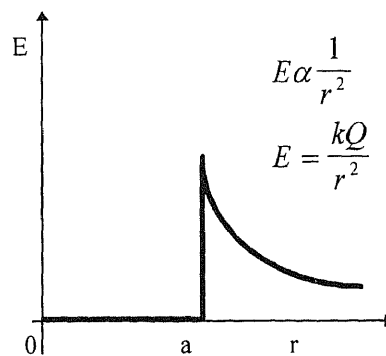
Figure 1.9 The relation between the electric field produced by a charged conducting sphere and its radius.(Inside the sphere the electric field is zero) [14].

The electric field produced by a charged conducting sphere of radius a obeys the inverse square law beyond the radius a and this relation is illustrated in Figure 1.9 [14]. The

electric field outside a conducting sphere is the same as that of a point charge at the center

of the sphere having the same value of Q. Inside the sphere, however, the field is zero (r:

distance from the center of a sphere; a: radius of the sphere).

1.5 Dipole of The Heart

In the electrocardiographic problem, the heart is viewed as an equivalent electrical

generator. The concept of the heart as a dipole generator originated with Einthoven in

1912 [12]. A common assumption is that, at each instant of time in the sequence of

ventricular activation, the electrical activity of the heart can be represented by a net

equivalent current dipole located at a point that is called the electrical center of the heart.

The dipole consists of points of equal positive and negative charge separated from one

another and denoted by the dipole moment vector M. Throughout the cardiac cycle, the

magnitude and direction of M, which is shown in Figure 1.10, vary because the dipole

field varies [18]. There have been several studies on the solution of the dipole position in

order to locate the site of electrical activity within the heart despite several

methodological limitations such as inhomogeneity of the human body, and variation of

individual body fluid [8]. It was reported that the moving dipole during the QRS wave

was within the small area in the region of the ventricle [9]. M. Nomura et al. [8] found

that in the normal subject, at the beginning of the QRS wave, the current dipole was

directed to the right and inferiorly due to the activation from left to right ventricle in the

intraventricular septum. After 40ms, the dipole was directed to the left mainly due to the
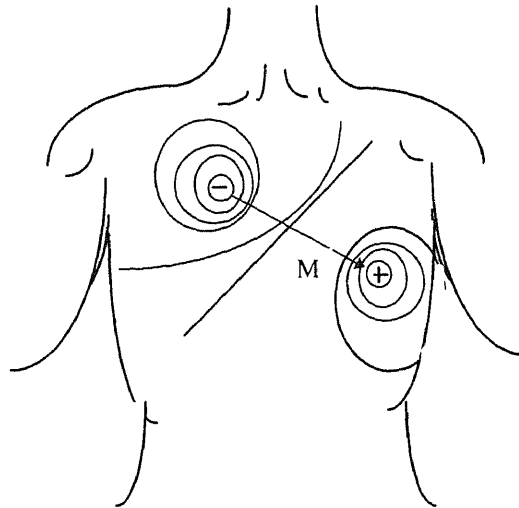
Figure 1.10 Rough sketch of the dipole field of the heart when R wave is maximal [18].

activation of the left ventricle. The rotation of the moving dipole was counterclockwise (Figure 1.11).

The change in the magnitude and orientation of the dipole causes a change in the electric field. Also, as mentioned previously, there is an attenuation of the electric field with increasing distance from the source. If the two electrodes are located on different equal potential lines of the electric field of the heart, a nonzero potential difference is
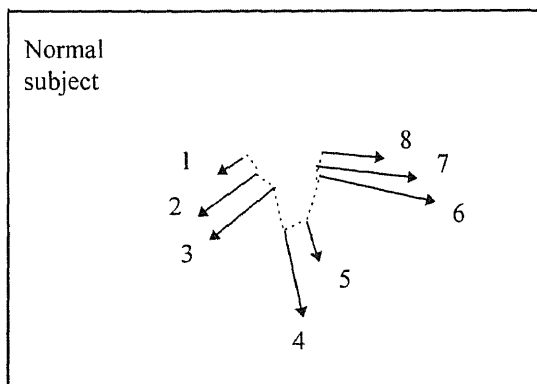
Figure 1-11 Single moving dipoles of a normal subject [8].

measured [18]. Different pairs of electrodes at different locations generally yield different

results because of the spatial dependence of the electric field of the heart.

CHAPTER 2

METHODS

The QT interval and QT dispersion were computed by means of an algorithm implemented using Labview. The results were statistically represented in terms of the mean and standard deviation. Also, the effect of the electric dipole of the heart on QT dispersion was investigated using the three limb leads.

Initially, single lead ECG signals were used to test the efficiency of the program for computing QT intervals. Afterwards, three limb leads were recorded simultaneously, and QT dispersion was computed and analyzed. The same process was repeated for four chest leads (V1 through V4) on two subjects. The QT interval of each of the channels was analyzed with respect to the mean and the standard deviation. To study the dipole effect of the heart on QT dispersion among three limb leads (Lead I, II, III), electrodes RA and LA were placed over the wrists outstretched and the other two (RL and LL) over the ankles (far field placements). Ten subjects with no history of heart disease were recruited to the study. All were males aged from 23 to 26 years. Near and far field measurements were taken, with five minutes of rest in between, for each subject while they were relaxed. Each ECG lead signal was recorded for one minute. The second part of the measurements were taken with the electrodes of RA and LA placed on the shoulders and the others below the chest cavity (near field placements). Near and far field measurements were taken with sampling frequency of both 200 Hz and 500 Hz separately. This was done to investigate the effect of the sampling frequency on the standard deviation. The resulting QT dispersion in far field measurements was expected

to be smaller than that in near field measurements because of the attenuating feature of the dipole electric field with increasing distance from the dipole center.

2.1 Data Acquisition

Two different ECG machines were used in taking measurements. While dealing with the four chest leads (V1 through V4) a BECKMAN R511A electrocardiograph machine was used. For the three limb leads a BECKMAN R611 ECG machine was used. These two ECG machines differ in the type of couplers they are using (Type 9876 and Type 9853A respectively). The couplers have different kind of input connectors. On each machine, "the preamplifier module" was set to 0.1 mV/mm and "the high frequency response" to 100 Hz for all channels. The multi-lead ECG signals with a frequency response of 0.5-100 Hz, were acquired by a 16 channel data acquisition board (AT-MIO-16L-25) with a sampling frequency of 200 Hz. Also, at the sampling frequency of 500 Hz, three channel ECG was acquired on ten subjects. The data was stored in a Pentium 166 computer system to be analyzed later by the LabView program.

2.2 Algorithm

To analyze the QT dispersion, an algorithm was developed which was composed of several steps :

- Preprocessing,

- QRS detection

- QRS onset and T wave end definition, and selection of possible noisy beats in order to remove them.

-

2.2.1 Preprocessing

After recording and storing the ECG, digital filters were applied to remove residual noise, motion artifact, 60 Hz line interference and then to make the detection of QRS onset and T wave end points easier.
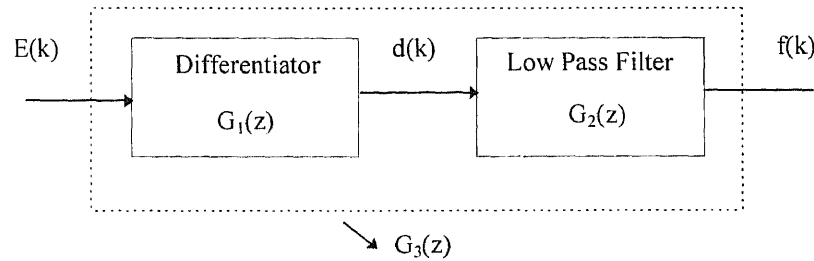
Figure 2.1 A block diagram representation of filtering steps.

Figure 2.1 shows in a block diagram the steps in filtering the ECG signal. E(k) represents the sampled ECG signal. This signal was passed through a differentiator filter block whose transfer function is defined as $G_1(z)$. The reason for using this differentiator filter is to obtain slope information for the QRS complex and then compute the QRS onset point using this information. In cases where the ECG signal has no Q wave, R wave location is used to determine the onset of the QRS complex. The transfer function of the differentiator filter is $G_1(z) = 1 - z^{-6}$ [15].

The output of the differentiated ECG signal is defined as d(k). The signal is then filtered with a first order low-pass filter to avoid residual noise and intrinsic differentiation noise. The transfer function of such an integer coefficient filter is $G_2(z) = \dfrac{1 - z^{-8}}{1 - z^{-1}}$ [15]. As can be seen from the frequency response, the filtering maximizes the energy of QRS complex between 10-15 Hz. Therefore it makes the detection of R wave peaks easy.

Fig.2.2 shows the frequency response of the differentiator $G_1(f)$, low-pass filter $G_2(f)$ and the combination of both which is $G_3(f) = G_1(f)G_2(f)$.
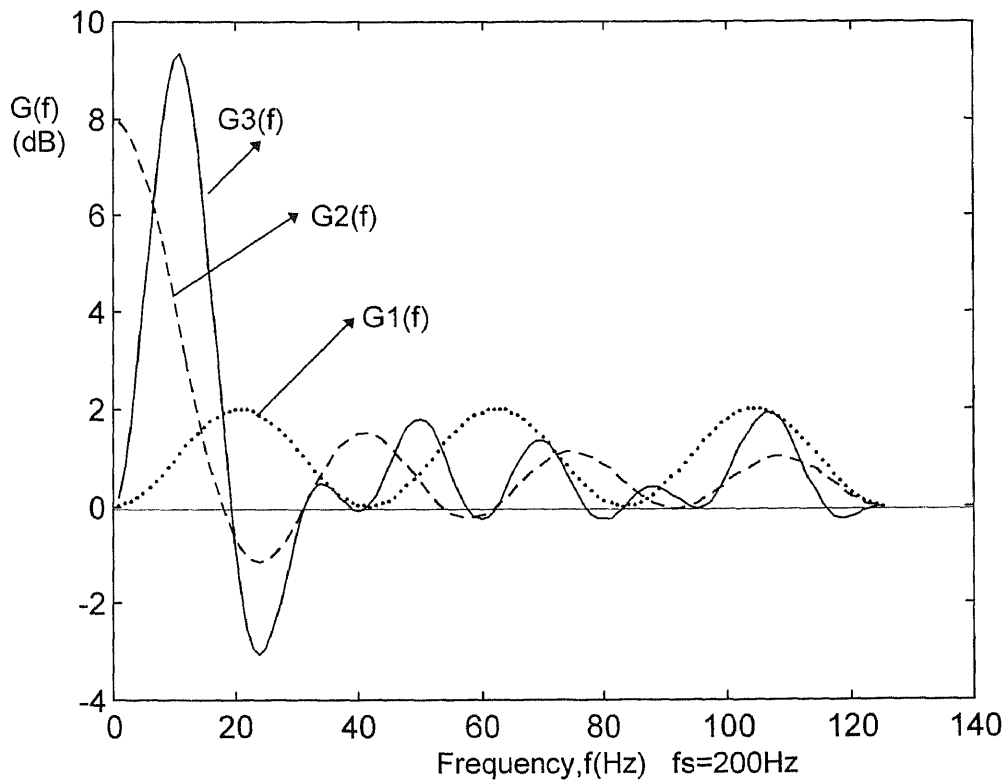
Figure 2.2 Frequency response of the filters G1, G2 and G3 at the sampling frequency of 200 Hz.

In the following discussion, f(k) is both the differentiated and low-pass filtered signal (See appendix A for more information on filters).

2.2.2 QRS Detection

After differentiating and filtering, an R wave detector was implemented based on an adaptive threshold. The algorithm also detects for a missing R wave. It readjusts the threshold and searches backward starting from the last detected R wave position, when the time interval between the two consequitive detected R waves is 1.8 times the average RR interval value. The detailed explanation of the algorithm is presented in appendix B.

2.2.3 R and Q Waves Definitions

In order to detect QRS onset and T wave end points, R wave location was the reference starting point. Therefore, R wave detector algorithm described previously was applied to the low pass filtered signal, f(k). The detected R wave points in the processed signal were defined as PK_n. These PK_n points were used to determine the Q and R waves on the ECG signal, E(k).

After detecting the PK_n points, the peaks of the highest slope both before and after PK_n were searched. The peak before PK_n was called PK_b and the peak after PK_n was called PK_a. Then, the absolute values of f(k) at points PK_a and PK_b were compared. If the absolute value of $f(PK_b)$ was greater than that of $f(PK_a)$, then R_p was determined as the zero crossing point preceding PK_n. Otherwise, Rp was defined as the zero crossing point following PK_n.

These R$_p$ points map onto the R wave peaks in ECG signal, E(k). The Q position Q$_p$ was defined as the zero crossing point preceding the Rp in the differentiated signal, d(k), not in the filtered signal, f(k), since the Q wave has high frequency components that can not be present in a low-pass filtered signal. This process is shown as a flowchart in Figure 2.3. Additional information about how this algorithm functions can be found in appendix B.
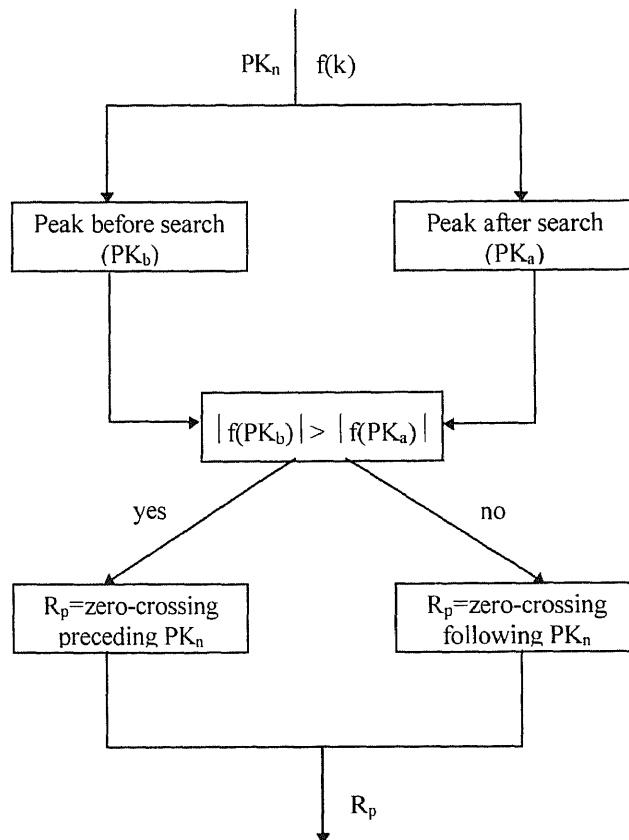
Figure 2.3 Flowchart to compute R_p points where the inputs are PK_n (detected peak) and f(k) (processed signal) [15].

2.2.4 QRS Onset Definition

The QRS onset (QRS_i) is defined as the beginning of the Q wave. To determine these points, the Q position Q_p and the R position R_p are required.
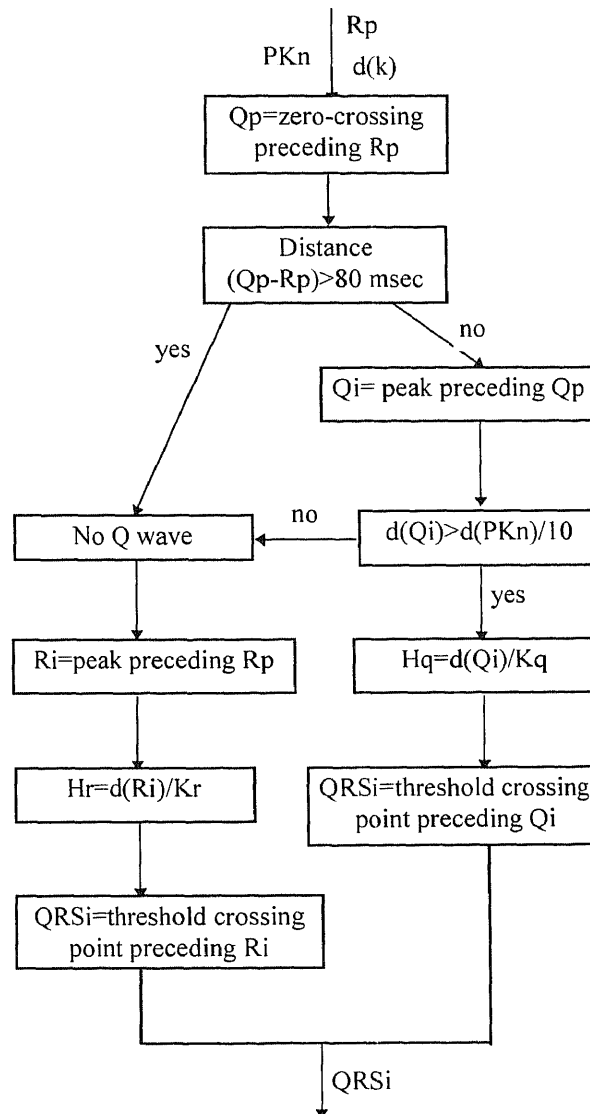
Figure 2.4: The Flowchart for QRS onset definition QRS_i, where the inputs are PK_n, R_p and d(k), that is the differentiated signal.

The implementation is shown in Figure 2.4. Starting from the Q_p point, a backward search was conducted for a point Q_i which is of a maximum slope in the differentiated signal d(k). Depending on the magnitude of this Q_i point, a threshold H_q was defined as the value of the differentiated signal at that point divided by a constant K which takes the value $K = K_q$ when the Q wave is present, and $K = K_r$ when no Q

wave is present. Then, QRS onset is defined as the backward threshold crossing point

starting from Q_i.

2.2.5 T Wave Peak and T Wave End Definition

From the R position, a search window was defined with limits bwind (beginning of the

window)and ewind (end of the window). The window size is variable which is decreased

when previous R-R interval decreases to avoid the coming P wave being detected as a

next T wave. If the average R to R interval is lower than 700ms, bwind is assigned 100ms

and ewind 0.7 RR_{av}. Otherwise bwind and ewind take the values of 140ms and 500ms,

respectively [15].

Four different kinds of T waves were defined according to the locations of the

maximum and minimum points between the limits of the window. First, the algorithm

makes a decision on the type of the T wave and apply a different detection process

specific to each type of the T wave This method increases the efficiency of the T wave

end detection process. The type of the T waves considered are as the following:

- Normal T wave (upward-downward)
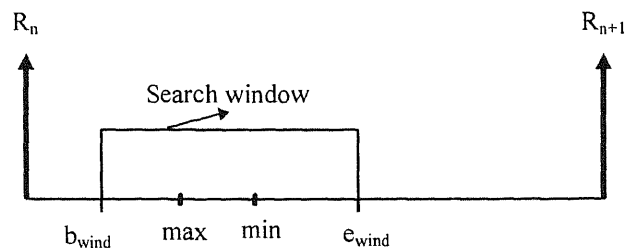
Figure 2.5 Illustration of a normal T wave.

As illustrated in Figure 2.5, R_n and R_{n+1} shows the detected R points consequently. Between the limits of the search window, if the maximum is before the minimum, the condition of "$|max| > 4|min|$" is checked. If it is false, the T wave is considered normal T wave (upward-downward).

- Only upward T wave

  If the condition above is true, then T wave is considered as only upward.

- Inverted T wave (downward-upward)

  If the min position is before the max position, then it is searched for the minimum (mina) between max and ewind (Figure 2.6). If $|max| < 4|min\,a|$, again the upward-downward T wave is considered. Otherwise, then next criteria, $|min| > 4|max|$, is checked. The true case makes the T wave inverted.

- Only downward T wave

  In Figure 2.6, If $|max| > 4|min\,a|$ and $|min| < 4|max|$, then it is considered as only downward T wave.

For more information on the T wave end detection algorithm, see appendix B. Figure 2.7 shows the flowchart for the T wave end detection procedure.
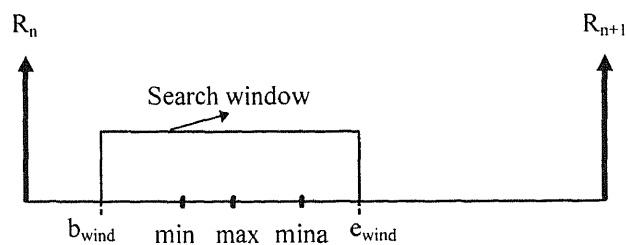
Figure 2.6 Illustration of a downward-upward T wave.

R_p f(k)

RR_{av}

$$RR_{av} > 700 \text{ ms}$$

No   Yes

bwind = 100 ms
ewind = 0.7 RR_{av}

bwind = 140 ms
ewind = 500 ms

Max and Min
search using f(k)
bwind and ewind

Criteria for T
wave shape

T_i definition

Threshold value
$H_t = f(T_i)/K_t$

Threshold
crossing point
following T_i

T_{end}
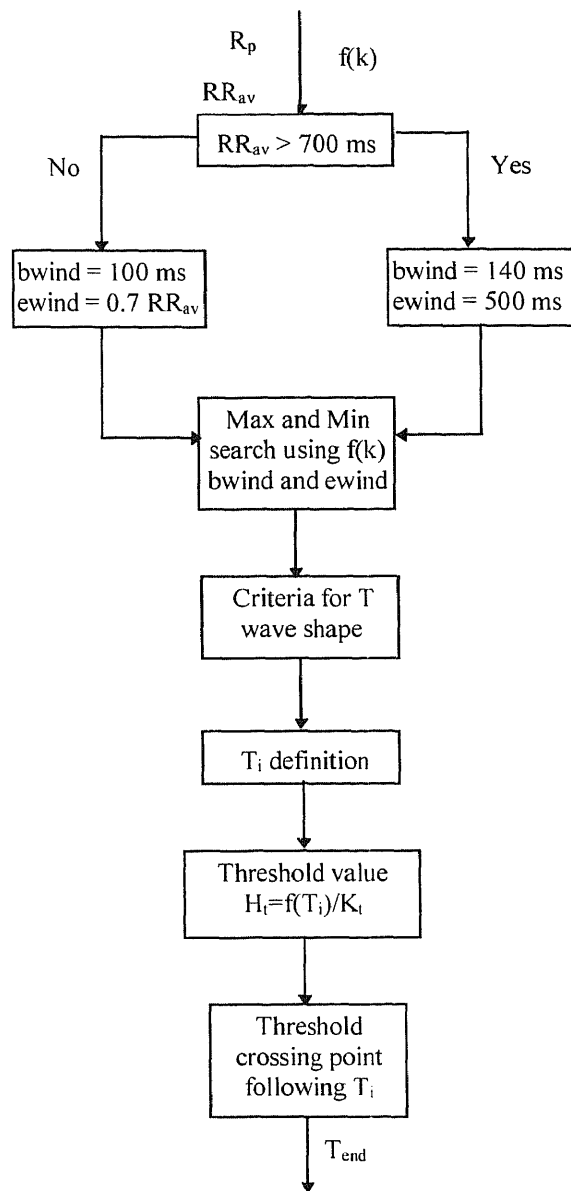
Figure 2.7 A Flowchart for T wave end definition [15].

2.2.6 Median Filtering

In previous studies, median filtering of either QT interval or QT dispersion to eliminate

any outlying was not encountered. Mode 3, the minimum limit, was chosen in this study.

The median filter works by taking every three points (mode 3 median filter) and

then assigning the one which has median value to the first point as a new value. This

process continues in order as illustrated in Figure 2.8. In this example, the fourth element of the array, 13, is taken out by the median filter. Also, it is seen that the length of the array after filtering is two less than that it was before filtering.

An algorithm was designed to apply median filtering to the QT dispersion array to eliminate unacceptable deviations from the mean. As can be seen from the Figure 2.9, any misdetected QT interval is removed from the resulting QT dispersion by means of the median filter. Figure 2.9(a) shows normal QTc interval array and Figure 2.9(b) the median filtered QTc interval array.
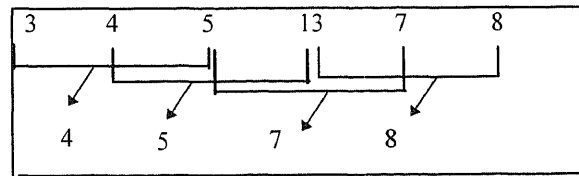
Figure 2.8 A simple illustration of a median filter of mode 3.

a) QTc interval array
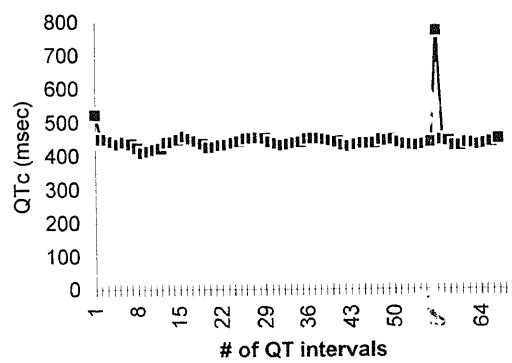
b) Median filtered QTc interval array
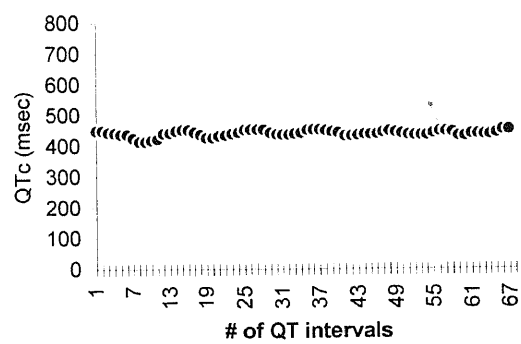
Figure 2.9 (a) Normal and (b) median filtered QTc arrays with mode 3 median filter.

CHAPTER 3

RESULTS

After designing the algorithm to detect QRS onset and T wave end points and then compute QT_c intervals, the reliability of the algorithm was first checked on a single channel recorded ECG signals. Also, the program was tested with three and four channel QT dispersion computation. Finally, the far and near field measurements were taken at different sampling frequencies (200 Hz, 500 Hz) and their possible effects were investigated the QT dispersion using three limb leads.

3.1 Single Channel Data Analysis

Twenty five 1 minute ECGs taken on normal subjects during rest, and stored on 1.44 floppy disks. The results are given in Table 3.1 in terms of the means and standard deviations of the QT_c intervals of each one minute ECG record.

Table 3.1 Computed QT_c intervals in terms of the mean and the standard deviation on 25 subjects.

	QT_c interval array			QT_c interval array	
	Mean	SD		Mean	SD
Subjects	msec		Subjects	msec	
1	454	26.61	14	454	10.90
2	449	9.40	15	448	7.53
3	461	8.53	16	439	8.40
4	460	10.10	17	447	11.41
5	460	10.91	18	440	4.33
6	458	9.26	19	441	4.45
7	449	4.80	20	400	4.53
8	450	8.88	21	417	5.84
9	451	15.51	22	437	15.14
10	450	15.39	23	431	9.34
11	449	15.79	24	395	6.79
12	446	15.64	25	395	5.89
13	430	7.55			

As can be seen from the Table, the mean QT_c interval values ranged from

460.79ms to 395.26ms. The mean of the QT intervals was taken among all the subjects

and it was 441.33ms. The results are also presented in a graphical form in Figure 3.1. The

standard deviations fluctuated mostly around 10. It was observed that for smaller mean

QT_c values, the standard deviations were smaller.
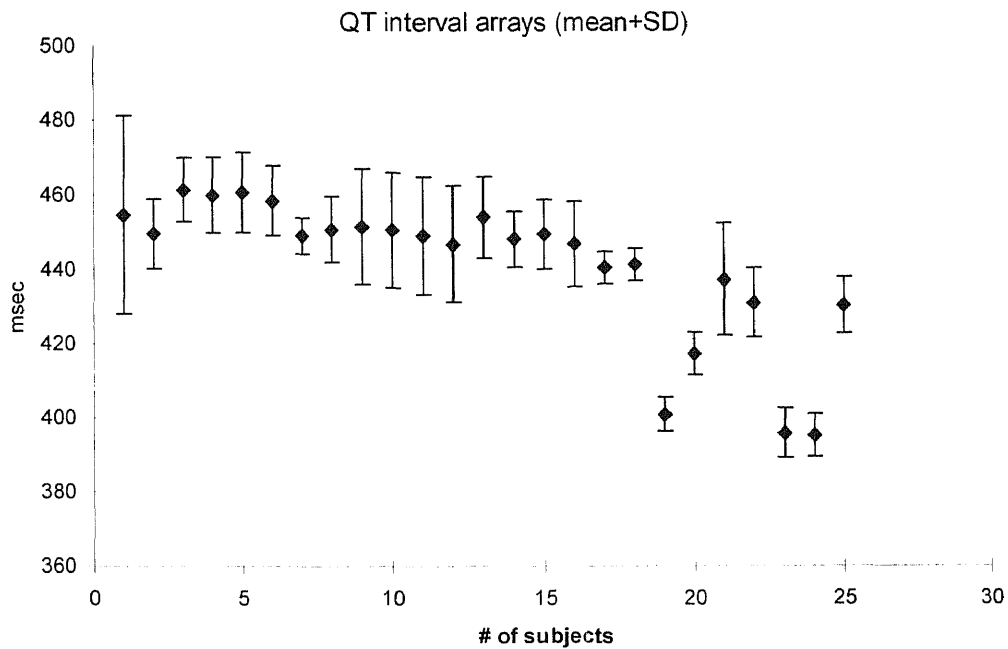
Figure 3.1 Computed QT intervals in the efficiency test of the algorithm.

Four of the ECG signals are shown together with the QRS onset and T wave end

detection points in Figure 3.2 (See appendix C for additional signals). Also, for each ECG

signal the QT_c intervals were plotted by means of the program (QTint.vi) written in

Labview.

ECG + (T end & QRS onset) points detected

median filtered QT interval array

1.8-
1.0-
0.0-
-1.1=
586   700   800   900   1000   1151

470.0-
460.0-
450.0-
440.0-
430.0-
0 10 20 30 40 50 60

mean 449.66   standart deviation 9.40

ECG + (T end & QRS onset) points detected

median filtered QT interval array

1.8-
1.0-
0.0-
-1.1=
892   1000   1100   1200   1300   14001457

480.0-
470.0-
460.0-
450.0-
440.0-
0 10 20 30 40 50 60

mean 461.34   standart deviation 8.53

ECG + (T end & QRS onset) points detected

median filtered QT interval array

1.8-
1.0-
0.0-
-1.1=
11441200   1300   1400   1500   1600   1709

490.0-
480.0-
470.0-
460.0-
450.0-
440.0-
0 10 20 30 40 50 60

mean 460.05   standart deviation 10.10

ECG + (T end & QRS onset) points detected

median filtered QT interval array

3.1=
2.0-
1.0-
0.2-
469   600   700   800   900   1035

480.0-
470.0-
460.0-
450.0-
440.0-
430.0-
0 10 20 30 40 50 60

mean 458.55   standart deviation 9.26

Figure 3.2 Outputs from the Labview program (QRS onset and T wave end detection points are present as well as the median filtered QTc intervals and their mean and standard deviations).(see appendix C for more).

When the plots of the QT_c intervals are examined, it is observed that the fluctuations of QT_c intervals look like sinusoid. This may be due to a respiratory effect. However, the signals were containing generally 5-7 cycles. At resting, the respiratory rate can not be in that range. There must be another effect to be investigated in future studies.

3.2 Three Lead Measurements

For one subject, three channel ECG signals (leads I, II, III) were recorded at the sampling frequency of 200 Hz for one minute and their QTc intervals and QT dispersions were computed. The measurement was repeated on the same subject. Results are given in Figures 3.3-3.6.
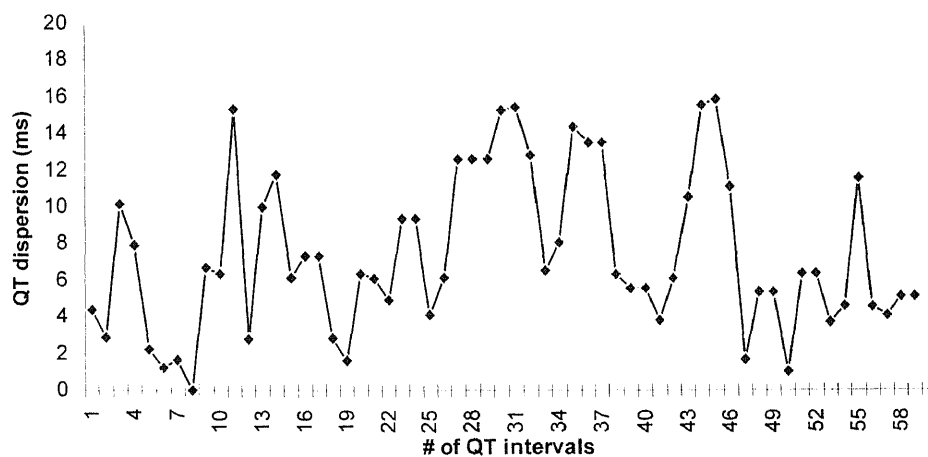
Figure 3.3 QT dispersion of leads I, II, III in one of the test measurements.

In Figure 3.3, the x axis shows the number of QT intervals during one minute of the recording and the y axis the resulting QT dispersion among three limb leads at each QT interval. The mean value of the dispersion was 7.42ms and the standard deviation 4.29. The QTc intervals of the individual leads (I, II, III) are shown in Figure 3.4. There

were no differences among the mean value of the 59 QTc intervals in lead I, II and III

(444, 443, 444ms respectively).
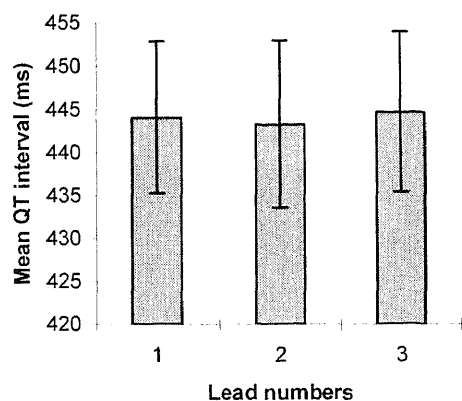
Figure 3.4 Mean QT_c intervals for each specific limb lead I, II, III.

Figure 3.5 shows the QT dispersion resulting from the second "three limb lead

ECG measurement".
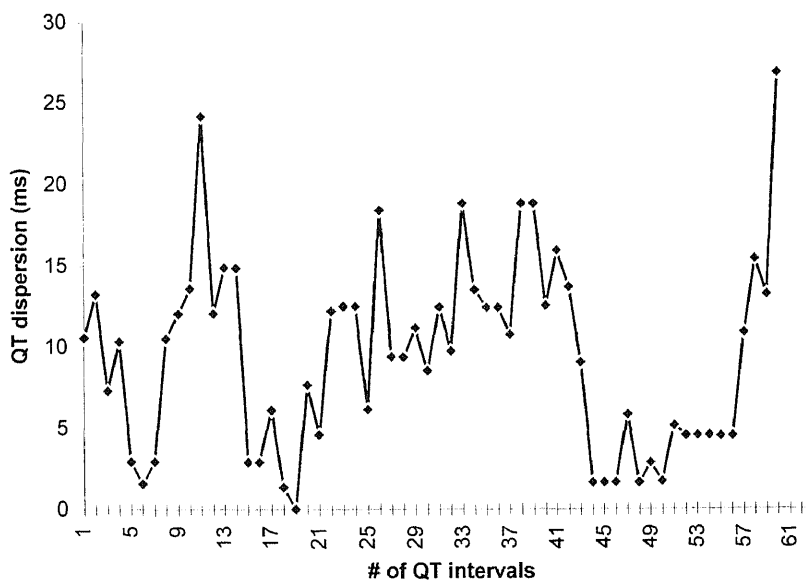
Figure 3.5 QT dispersion of lead I, II, III in another test measurement.

The dispersion fluctuated between 0ms and 34ms. The mean was 9.28ms and the SD (standard deviation) 5.93ms. The QTc intervals for each lead had the same mean value, 434ms, as shown in Figure 3.6.
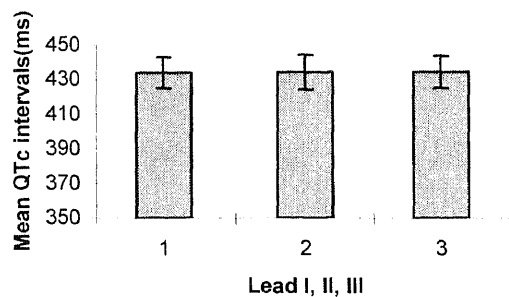
Figure 3.6 Mean QTc intervals of lead I, II, III.

3.3 Four Lead Measurements

In four lead QT dispersion test measurements, the first four chest leads (V1, V2, V3, V4) were recorded at 200 Hz twice on the same subject. The mean QT dispersion was 7.01ms and the standard deviation of the dispersion 2.97ms. Figure 3.7 shows the four lead QT dispersion curve.
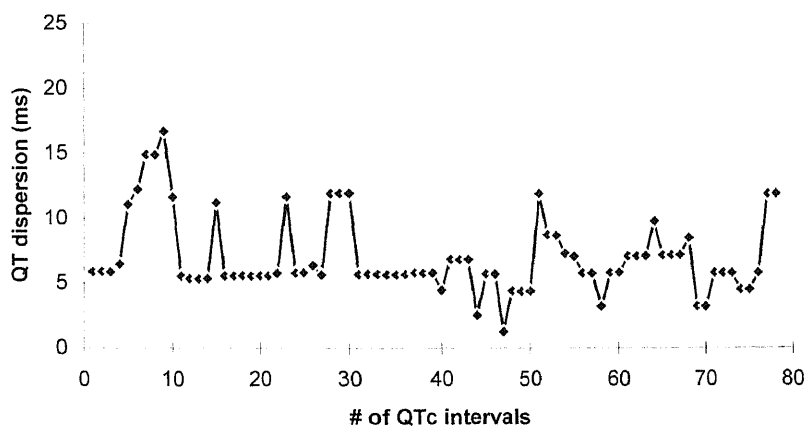
Figure 3.7 QT dispersion of lead V1 through lead V4.

The x axis contains the numbers assigned to each QT_c interval, and the QT dispersion is plotted on the y axis. It was observed that lead V4 had the highest mean QT interval with the value of 388.21ms and lead V3 the lowest mean value of 382.73ms. The mean QT_c intervals of the leads are shown in Figure 3.8, together with the standard deviations.
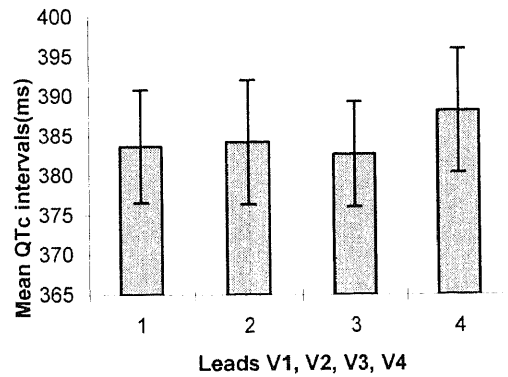
Figure 3.8 Mean QTc intervals of leads V1 through V4.

The second four lead QT dispersion measurement on the same subject also produced the same results (Figure 3.9).
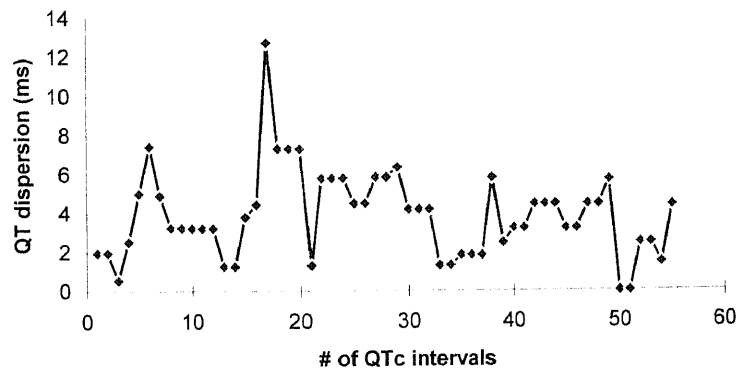
Figure 3.9 QT dispersion of the leads V1 through V4.

The mean QT dispersion was 3.87ms, but the standard deviation was 2.24. Lead V4 showed the highest mean QT interval (386.43ms), and the smallest mean value was encountered in lead V3.as shown in Figure 3.10.
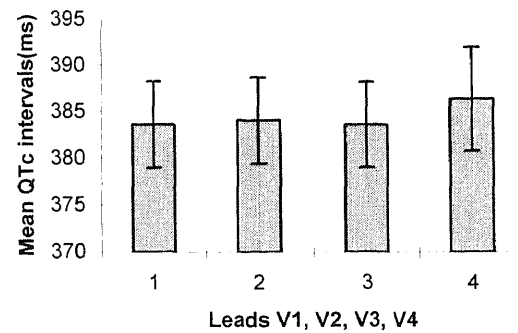
Figure 3.10 QT dispersion of the leads V1 through V4.

3.4 Far and Near Field Measurements

In order to investigate the near and far field effect of the electric dipole of the heart on QT dispersion, the three limb lead measurements were taken at different electrode locations as described in section 2.

Table 3.2 Near and far field mean QTc intervals and the mean QT dispersion of three limb leads at the sampling frequency of 200 Hz ($P<0.05$).

Subject	near /far	mean I	SD I	mean II	SD II	mean III	SD III	mean (disp)	SD (disp)
		msec		msec		msec		msec	
I	near	387	9,81	388	11.01	389	11.48	9.54	5.77
	far	368	8.08	367	5.66	366	7.78	9.53	5.39
II	near	386	7.21	386	7.22	389	10.14	6.19	6.19
	far	372	6.89	371	8.31	375	10.12	3.26	4.17
III	near	383	7.68	383	7.65	382	12.70	7.90	6.07
	far	370	6.27	370	6.17	371	6.55	3.82	3.06
IV	near	384	13.09	380	5.42	380	4.43	11.17	6.61
	far	374	6.05	374	6.25	374	7.11	2.30	2.19

First, the data were recorded at the sampling frequency of 200 Hz. on four different subjects.The results in terms of the mean of the all QT_c intervals of each lead and the mean QT dispersion are shown in Table 3.2 along with the standard deviations.

The columns (mean-SD I, II, III) present the mean and the standard deviation of the QTc intervals of each lead. The last two columns include the mean and SD values for the resulting QT dispersions.

For the first subject, the mean QT dispersion for the far field measurement was 9.54ms which was higher than the QT dispersion for the near field measurement. For the other three subjects, the QT dispersions were higher for the near field measurements (6.19ms, 7.90ms, 11.17ms) than those for the far field (3.26ms, 3.82ms, 2.30ms). However, the standard deviations of the dispersions were quite large. Therefore, thinking that an increase in the sampling frequency might decrease the SDs, the measurements were repeated at 500 Hz sampling frequency and for more subjects. The results are shown in Table 3.3.

In the "Subject" column, each subject was described by a different letter. As shown in the table, the mean of the QTc intervals among the subjects varied between 343ms and 390ms. The QT dispersions for the far field measurements were slightly smaller than those for the near field measurements except for subjects E1, I and J2.

Table 3.3 The QTc intervals and QT dispersions of near and far field measurements
at the sampling frequency of 500 Hz (p<0.05).

Subject	near /far	mean I	SD I	mean II	SD II	mean III	SD III	mean (disp)	SD (disp)
		msec		msec		msec		msec	
A	near	355	6.50	349	6.74	354	7.59	7.63	5.45
	far	356	5.46	357	5.18	357	5.18	7.01	3.56
B	near	355	7.01	354	6.98	351	7.91	8.38	5.58
	far	344	5.05	343	7.44	344	5.35	6.29	4.03
C	near	363	5.81	363	6.12	362	7.06	7.35	3.28
	far	348	5.72	358	10.28	349	5.57	6.82	4.17
D	near	386	6.08	386	6.62	388	6.57	7.08	4.96
	far	378	5.91	379	6.13	382	5.98	6.83	4.17
E1	near	379	15.65	378	11.82	377	11.13	9.58	6.02
	far	379	11.44	378	12.02	377	13.40	10.42	8.10
E2	near	377	5.76	377	5.64	371	15.86	12.71	8.35
	far	376	12.31	377	12.04	374	11.05	9.74	7.62
F	near	364	11.11	366	10.87	361	17.64	10.69	7.82
	far	360	8.51	361	9.61	356	11.69	9.66	6.61
G	near	368	15.15	370	15.08	366	15.56	10.61	6.03
	far	379	10.57	380	10.01	376	9.21	8.42	5.21
H	near	365	7.15	365	8.01	369	16.02	16.40	9.67
	far	365	8.18	367	11.43	359	13.75	14.97	9.79
I	near	370	5.97	370	5.72	371	12.31	10.30	6.40
	far	367	7.17	366	7.32	365	11.48	11.51	8.41
J1	near	363	8.99	361	8.02	358	14.66	11.87	7.16
	far	360	10.92	360	9.92	357	13.75	11.40	8.05
J2	near	364	7.16	364	6.57	358	8.54	11.33	8.83
	far	360	5.96	359	8.24	358	13.69	12.45	7.75

In Figure 3.11, the QT dispersions for each subject in both cases are shown with
two adjacent bars. In each group of bars, the first shows the near field QT dispersion and
the second the far field QT dispersion. It is seen that in most of the cases near field
measurements were slightly higher.
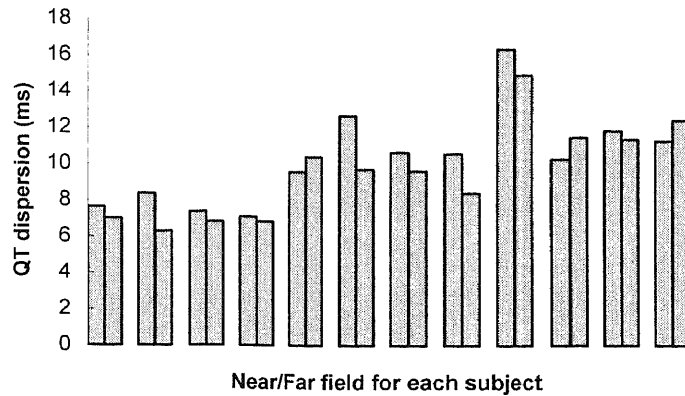
Figure 3.11 QT dispersions in near and far field measurements respectively for each of the 12 subjects.

In addition, the T test was applied between far and near field measurements at 500 Hz sampling frequency to support the results from a statistical point of view. Null hypothesis, H_0 , means that there is no difference between the population means of the near and far field measurements. On the other hand, alternative hypothesis, H_1, assumes that there is a difference between the population means of the two groups on the test of near and far field effect. The "t" was found as 1.822 for 22 degrees of freedom (p<0.05). The degrees of freedom, df, is equal to 2(n-1) where n is the number of measurements taken. The critical value is 2.074 for 22 degrees of freedom. Since, the obtained t falls within the region smaller than 2.074, the hypothesis H_1 is rejected. The result of the T test showed that the near and far field mean QT dispersions were statistically not different. It means both samples were drawn from the same population.

CHAPTER 4

DISCUSSION

4.1 Measurements to Test the Algorithm

The algorithm designed to compute QT interval and dispersion was applied to the twenty five single lead ECG measurements. The computed overall mean QTc intervals was 441ms with the mean standard deviation of 10ms. In the literature, the mean values of QTc intervals varied from 367 ± 62ms to 448 ± 39ms [19,5]. Compared to these values in terms of standard deviations, the results of the present algorithm was smaller. The standard deviation among the measurements in the present study never exceeded 16ms, except for 26.61ms from one subject. That is the distribution was around 10. The detected QRS onset and T wave end points were checked to find a possible reason for the high standard deviation. It was found that the high SD was not caused by misdetection. It might be patient dependent rather than algorithm itself.

In Figure 3.2 in section 3, the QRS onset and T wave end points detected by the algorithm are shown together with the ECG signals themselves. These outputs prove that the algorithm is very accurate for different types of ECG signals such as those with T wave amplitudes higher than those of the QRS waves, as well as ECG signals with motion artifact. They can be seen in plots in appendix C.

In QT interval measurements, it was also observed that the QT interval curves had sinusoidal fluctuations. These shapes may have resulted from the respiration rate of the subject. However, the number of the cycles in one minute QT interval was changing from 5 to 7. At resting, the respiratory rate is supposed to be between 12-16 per minute Since

the respiration rate was not measured in the present study and there is no evidence in the past studies, further studies should be performed to be able to assert that kind of effect.

In three lead QTc interval and dispersion measurements, lead III has the higher mean QTc interval values than leads I and II. However, the difference was mostly less than 3ms. The dispersion was found as 7.65 ± 4.61ms. In one of the past studies [25], the QT dispersion was computed as 40ms among just three limb leads, the result here was smaller. Since the QT dispersion among 12 leads was found generally less than 40ms [20,5,19], the dispersion of leads I, II, III should be lower than 40ms. This is logical since in the 12 lead QT dispersion, at a specific beat interval, some of the maximum and minimum QT intervals came from the six chest leads. Another research result supports this proposal. In 12 lead unadjusted ECG data set the QT dispersion was found to be 46.2 ± 20.8ms [20]. On the other hand, the dispersion was 34.9 ± 21.1ms in the 6 precordial leads [20]. The QT dispersion for several beats per subject and the mean QT dispersion among all the subjects were computed. The numbers above reflects the mean and standard deviation of the dispersion among the subjects not the mean and the SD of the QT dispersion computed from the measurements taken on single subject as in the present study. For that reason, the mean and standard deviations found in the present study turned out to be smaller. In the literature there is no similar study to compute QT dispersion, so no result could be encountered as a comparative tool to the current study.

As for the four lead QT dispersion measurements, it was conducted on just two subjects. It is difficult for that reason to analyze the results statistically. The dispersions were 7.01 ± 2.97 ms and 3.87 ± 2.24ms in these two measurements. Compared to the three

limb lead measurements, it can be said that the dispersion among the leads V1 through V4 was smaller.

4.2 Near and Far Field Effect Measurements and Analysis

The first set of measurements were made at a sampling frequency of 200 Hz. The resulting standard deviations were quite large compared to the mean values of QT dispersions. The maximum mean QT dispersion was 11.17ms and occurred in near field measurements and the minimum was 2.30ms which occurred during far field measurements. In this study it was hypothesized that the far field measurements results in lower QT dispersions than near field measurements because of the attenuation of the electric field effect of the moving dipole with increasing distance from the dipole center. The results support the above hypothesis. However, the high SDs made it necessary to take the measurements at the higher sampling frequency of 500 Hz. The increase in the sampling frequency didn't markedly affect the deviations but the difference between near and far field mean QT dispersions decreased. In nine out of twelve cases, the mean QT dispersion for the near field was slightly higher than that for far field.

To support the results from a statistical point of view, the T test was applied to the mean QT dispersions between far and near field measurements. The T test is used to compute the probability of being wrong. Null hypothesis, H_0 , means that there is no difference between the population means of the near and far field measurements. On the other hand, alternative hypothesis H_1 assumes that there is a difference between the population means of the two groups on the test of near and far field effect [7]. If T is

smaller than the critical value it is concluded that the data are compatible with the hypothesis that both samples were drawn from a single measurement, that is the near and far field measurements do not differ. In the present study, the T value was 1.822. T did not exceed the 5 percent value of 2.074 for 22 degrees of freedom. Hence, there was not strong evidence to assert that near and far field mean QT dispersions were statistically different. Therefore, the hypothesis H_1 was rejected. The standard deviations of the measurements were very high compared to the mean values. Therefore, the result of the T test that the data were drawn from a single population was not surprising. Possibly, if the number of the subjects were higher, (25-30), a different result might be obtained.

CHAPTER 5

CONCLUSIONS AND FUTURE STUDIES

The algorithm to compute QT intervals is efficient in detecting QRS onset and T wave end points. It can be used in future multilead QT dispersion analysis studies. The main limitation of this study was the population. The number of subjects in near and far field investigation measurements was 10. If the number of subjects was higher, the results concluded statistical results might be different.

The followings are the conclusions from the various measurements:

- The mean QT intervals were within the same range as those in past studies [19, 5, 20, 23]. Also, the present algorithm produced smaller standard deviations.

- In near and far field measurements the increase in the sampling frequency from 200Hz to 500Hz did not result in a statistical difference for the mean and standard deviation of the QT dispersion measurements.

- There is no statistical difference between the near and far field QT dispersions. In other words, near and far field electrode locations did not affect the resulting QT dispersion. The increase in the number of the subjects may be a factor to affect the T test result.

The present study was just an introduction to the future studies, in terms of analyzing three lead QT dispersion. Using twelve channel QT dispersion is a feature of next studies.

The algorithm designed here will be used in a future study to investigate cardiac rate variability and repolarization dispersion in newborn infants by means of noninvasive electrocardiographic recordings and computer analysis of heart rate variability repolarization dispersion. QT dispersion will be measured for multiple leads (8-12 more than 1 or 2 beats (throughout one minute) Moreover, frequency analysis o dispersion like R_R variability studies will be performed. This study will be realiz collaboration of Dr. Levine from UMDNJ.

APPENDIX A

DIFFERENTIATOR AND LOW-PASS FILTER

The differentiator filter, d(k):

The transfer function: The differential equation:

$$G_1(z) = 1 - z^{-6},$$
$$|G_1(wT)| = 2|Sin(3wT)|,$$

y(nT)=x(nT)-x(nT-6T),

T is the sampling period and the gain is 6T.

The slope of the R wave is a popular signal feature used to locate the QRS complex [13]. A derivative algorithm that provides slope information is straightforward to implement. For that reason, six point derivative filter shown above was used.

The first order low-pass filter, f(k):

The transfer function: The differential equation:

$$G_2(z) = \frac{1 - z^{-8}}{1 - z^{-1}},$$
$$|G_2(wT)| = \left|\frac{Sin(4wT)}{Sin(wT/2)}\right|,$$

y(nT)-y(nT-T)=x(nT)-x(nT-8T),

the DC gain is 8 and the cut-off frequency at -3dB is about 20 Hz.

The band-pass filter, G₃(f)

The bandpass filter, $G_3(f) = G_1(f)G_2(f)$, reduces the influence of muscle noise, 60 Hz interference and baseline wander. The desirable bandpass to maximize the QRS energy is approximately 10-15 Hz [13]. It is true to say that 60 Hz line interference is quite minimized and QRS energy maximized so that R point detection gets easier.

APPENDIX B

QT INTERVAL ALGORITHM

Detailed explanation of an R wave detection algorithm:

First, two seconds of ECG data is searched for the highest negative or positive peak. The absolute value of this initial peak PK_1 is multiplied by a variable coefficient whose default value is 0.7 to determine the initial threshold (H_1). Then, a QRS is detected as the first maximum or minimum whose absolute value is larger than H_1.

PK_n denotes the maximum absolute value of the QRS at the nth beat in the processed signal f(k). The next threshold H_{n+1} is calculated as

$$H_{n+1} = 0.7H_n + 0.3(0.7PK_n)$$

The coefficients 0.7 and 0.3 are programmed to be adjustable values to make the detection process easier for some noisy and distorted ECG signals. Moreover, a recursive backward search is outfitted for missing beats, with a lower threshold which is 0.85 times smaller than the current threshold, when the next beat is farther than 1.8 times the last R-R interval.

P. Laguna et. Al [23] used the same kind of algorithm to detect R waves.

Detailed explanation about Q and R wave definition algorithm:

After detecting the PK_n points in the processed signal the nearest backward or forward peak is searched. It is known that the R wave has the highest slope in the QRS complex; thus PK_n will be the maximum slope value on either the upward going side or downward going side of the R wave.
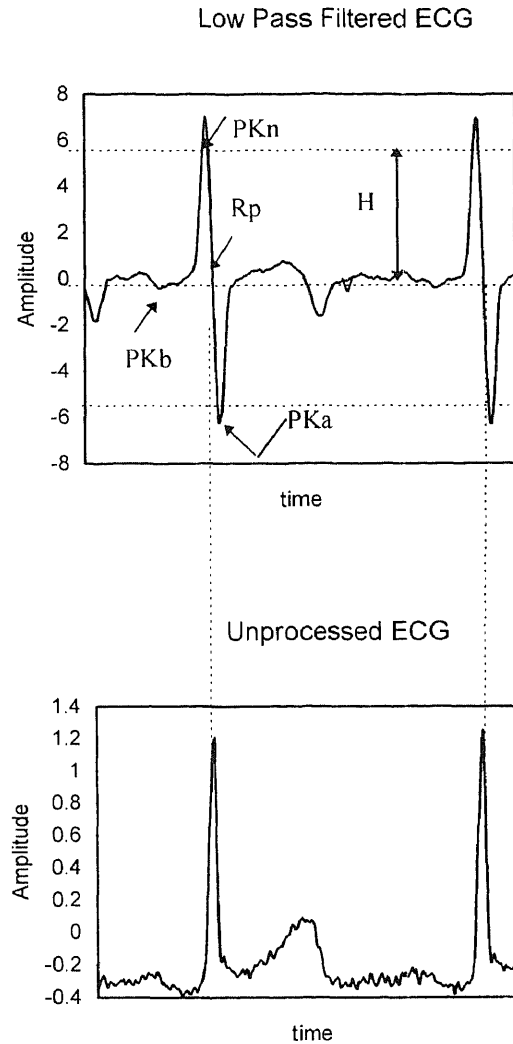
48

Low Pass Filtered ECG

Unprocessed ECG

Figure B-1 The output of the low-pass filtered ECG and the original ECG. (The threshold H and other specific points PK_n, PK_a, R_p are shown as described in the text.)

Depending which has the larger absolute value, the R position R_p is chosen as the zero crossing between PK_n and the peak of highest absolute slope. Figure B-1 shows the specific points described before.

The Q position Q_p is defined as the zero crossing preceding the R_p position in the differentiated signal, d(k). It is not in the filtered signal because the Q wave has high

frequencies that are not present in a low-pass filtered signal. When the R_p-Q_p interval exceeds 80 ms no Q wave is considered. This generally occurs when no Q wave is present.

T wave end detection algorithm:

A search is done for the maximum and minimum values of the processed signal, f(k) between the limits of the defined window as shown in Figure B-2. The statement limits of the window which are bwind and ewind is as follows:

If
RR_{av} > 700ms
(bwind, ewind) = (140, 500)ms,
then else
(bwind, ewind) = (100, 0.7RR_{av})ms
end

The shape of the T wave is decided with the following criteria:

If the maximum position is before the minimum position, then the T wave may be upward-downward or only upward; to characterize the only upward T wave, the selected condition is $|max| > 4|min|$.

If the minimum position is before the maximum position, a minimum is searched which is named min_a between the max position and the end of the window. If min_a is comparable in absolute value with the maximum, again the upward-downward T wave is considered. Otherwise, T only-downward is decided.

Unprocessed ECG

Amplitude

1.4
1.2
1
0.8
0.6
0.4
0.2
0
-0.2
-0.4

T wave end

time

Low Pass Filtered ECG

8

6

4

2

f(k)   0

-2

-4

-6

-8

ewind

bwind

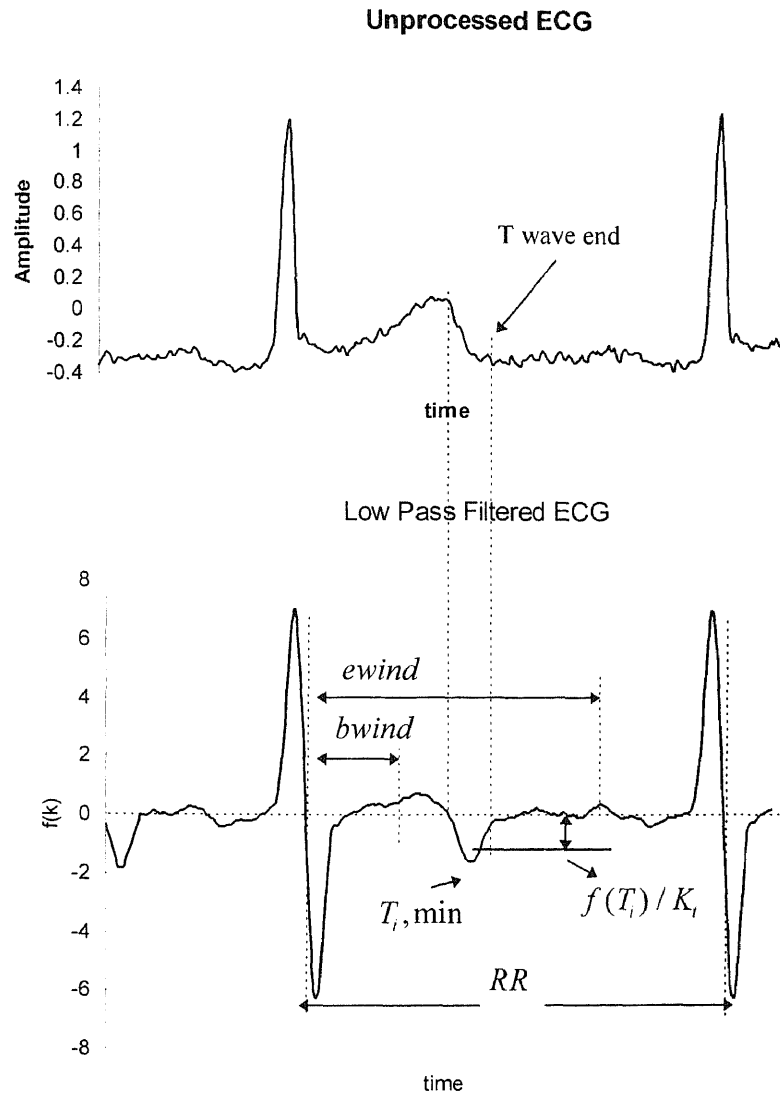T_i, min

$f(T_i)/K_i$

RR

time

Figure B-2 The original and processed ECG signals. In the processed signal the T wave end definition is described where bwind is the distance from the R position to the beginning of the search window, and ewind is the distance from the R position to the end of the window.

With these considerations, the last highest slope point of the T wave, T_i is defined. Afterwards, starting from T_i, the T wave end point is searched in the following way: the value of the processed signal, f(k), at the point T_i is denoted as $f(T_i)$. This value carries

the information pertinent to the T decay rate. The T wave end point is defined in such a

way that the downward processed signal reaches a threshold value H_t at a

$H_t = f(T_i) / K_t$, where K_t is an experimental value that the algorit

best. Laguna P. et. al. had used "2" for K_t in their study in 1990 [23]. I

value is chosen as "2.5". In the algorithm, when the T wave has a highe

value, $f(T_i) / K_t$ also has a higher or lower value to reach the T wave

frequency baseline interference has great importance in methods f

definition based on baseline considerations [17]. In the method used here

influence, because these baseline interferences are of lower frequency th

wave, and the differentiator has very poor gain for these frequencies in

its gain for T wave frequencies.

APPENDIX C

ECG SIGNALS WITH DETECTED POINTS

Below are the outputs from the Labview program (QRS onset and T wave end

detection points are presented as well as the median filtered QTc intervals and their
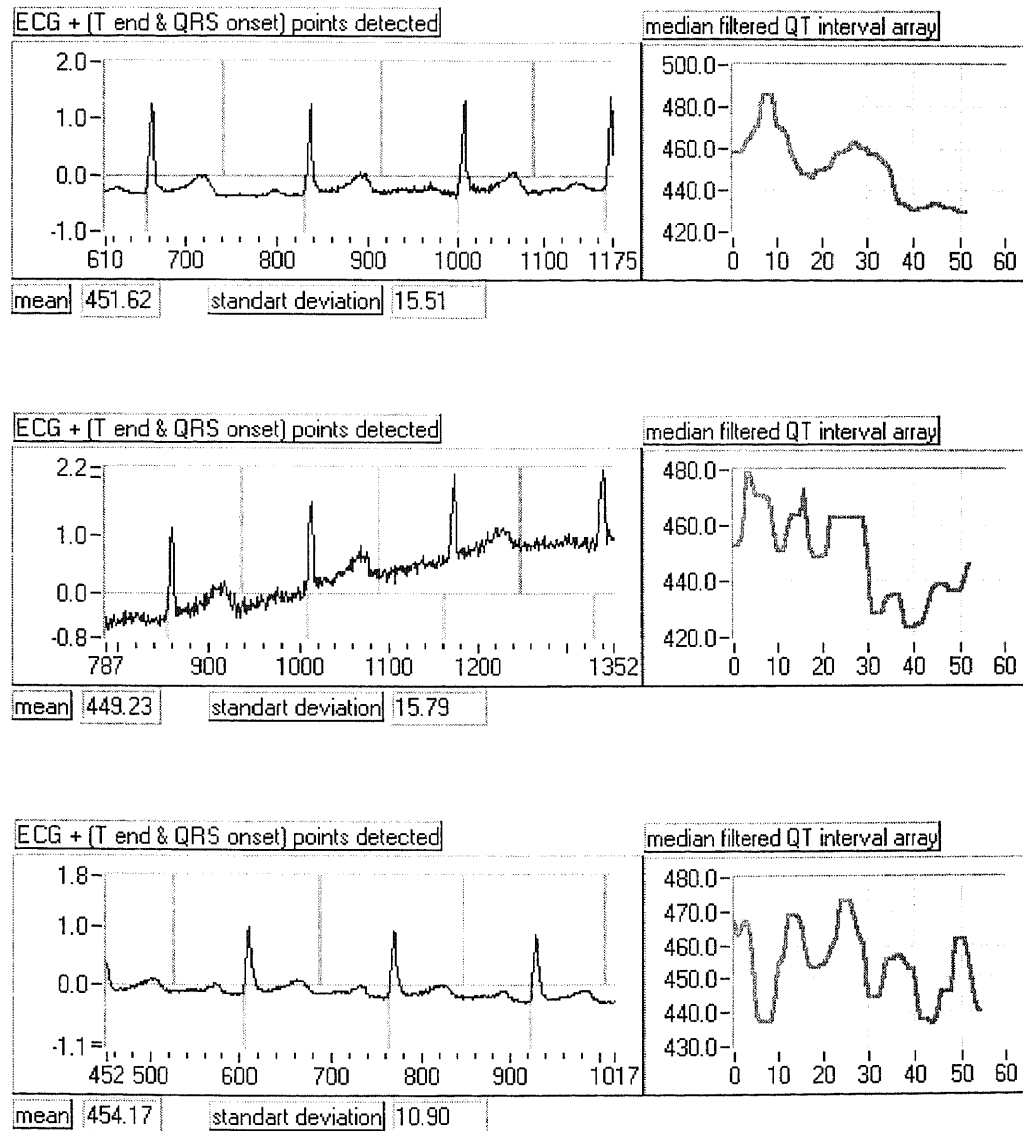
mean and standard deviations).

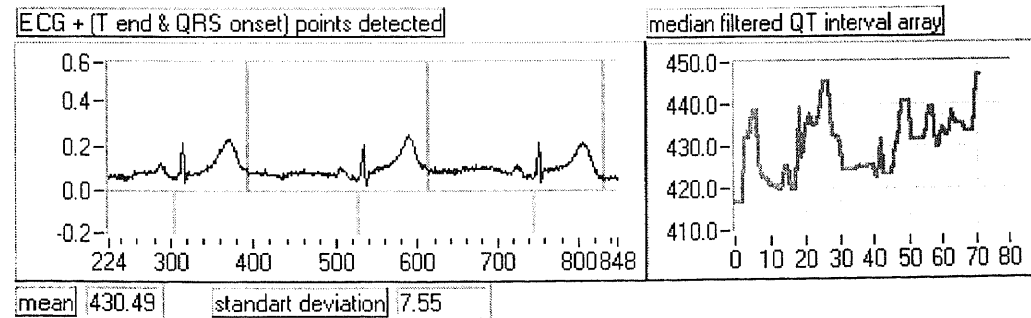**Figure C.1** Data outputs computed by LabView program.

ECG + (T end & QRS onset) points detected | median filtered QT interval array

mean 448.30 | standart deviation 7.53

ECG + (T end & QRS onset) points detected | median filtered QT interval array

mean 447.01 | standart deviation 11.70

ECG + (T end & QRS onset) points detected | median filtered QT interval array

mean 400.88 | standart deviation 4.53

ECG + (T end & QRS onset) points detected | median filtered QT interval array

mean 430.49 | standart deviation 7.55

Figure C.1 Continued .

ECG + (T end & QRS onset) points detected

median filtered QT interval array

mean 431.09   standart deviation 9.34

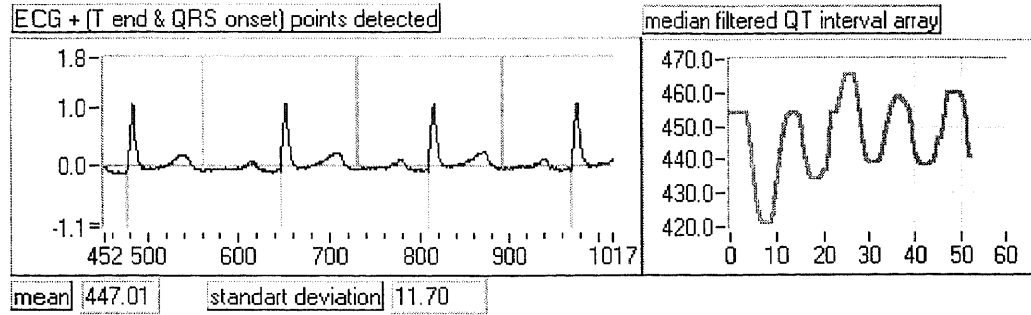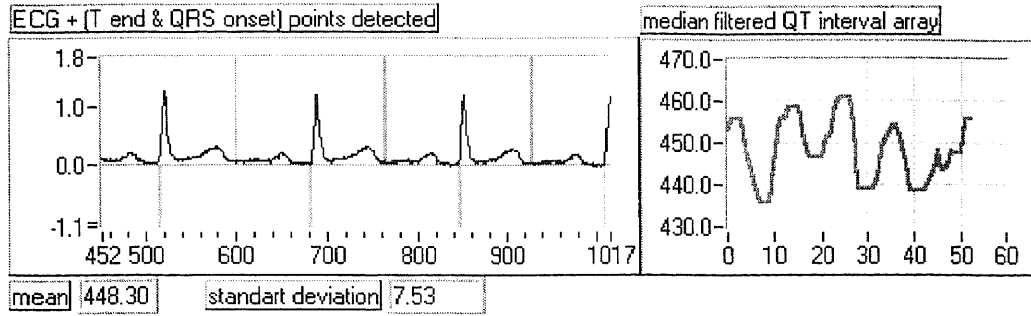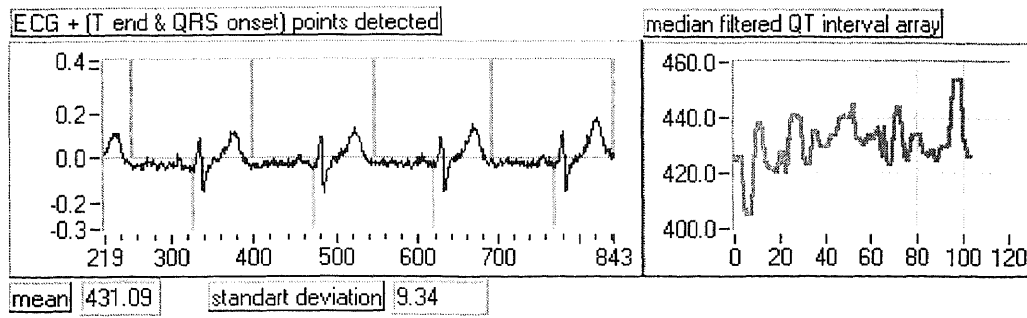**Figure C.1** Continued

REFERENCES

[1]. J. Molnar, " Evaluation of five QT correction formulas using a software-assisted method of continuous QT measurement from 24-hour Holter recordings," *American Journal of Cardiology*, vol. 78, pp. 920-926, 1996.

[2]. *Eletrocardiographic Text Book*, American Heart Association, vol. 1, pp. 156-157, TX, 1957.

[3]. J. Morganroth, F. V. Brozovich, J. Mc Donald, R. A. Jacobs," Variability of the QT measurement in healthy men, with implications for selection of an abnormal QT value to predict drug toxicity and proarrhythmia," *The American Journal of Cardiology*, vol. 67, pp. 774-776, 1991.

[4]. M. M. Laks," Long QT interval syndrome. A new look at an old electrocardiographic measurement- the power of the computer," *Circulation*, vol. 82, pp. 1539-1541, 1990.

[5]. J. S. Perkiomaki, M. J. Koistinen, S. Yli-Mayry, H. V. Huikuri," Dispersion of QT interval in patients with and without susceptibility to ventricular tachyarrhythmias after myocardial infarction," *The Journal of American College of Cardiology*, vol. 26, pp. 174-178, 1995.

[6]. J. Mayet, M. Shahi, K. Mc Grath, N. R. Poulter, P. S. Sever, R. A. Foale, S. M. Thom," Left ventricular hypertrophy and QT dispersion in hypertension," *American Heart Journal*, vol. 28, n. 5, pp. 791-796, November 1996.

[7]. S. A. Glantz, *Primer of Biostatistics*, Mc Graw Hill Company, MA, 1987.

[8]. M. Nomura, K. Nakayasu, Y. Nakaya, Y. Miyoshi, T. Wakatsuki, K. Saito, S. Bando, S. Ito," Single moving dipole obtained from magnetic field of the heart in patients with left ventricular hyperthropy," *Clinical Cardiology*, vol. 15, pp. 752-758, 1992.

[9]. R. M. Arthur, D. B. Geselowitz, S. A. Briller, R. F. Trost," The path of the electrical center of the human heart determined from surface electrocardiogram," *Journal of Electrocardiology*, vol. 4, pp. 29-33, 1971.

[10]. D. M. Mirvis, " Spatial variation of the QT intervals in normal persons and patients with acute myocardial infarction," *Journal of American College of Cardiology*, vol. 5, pp. 625-631, 1985.

[11]. R. Ashman," The normal duration of the QT interval," *Heart*, vol. 23, pp.522-534, 1942.

[12]. M. Mednegy, Z. Antaloczy, Z. Cserjes," A new possibility in the study of heart activation: the nondipolar body surface map," *Canadian Journal of Cardiology*, vol. 9, n. 3, April, 1993.

[13]. J.Pan, W. J. Tompkins," A real time QRS detection algorithm," *IEEE Transactions on Biomedical Engineering*, vol. 32, n. 3, March 1985.

[14]. S. A. Marantz, *Physics*, Benziger Inc, NY, 1969.

[15]. P. A. Lynn," Online digital filters for biological signals, some fast designs for a small computer," *Medicine and Biological Engineering*, vol. 15, pp. 534-540, 1977.

[16]. A. J. Vander, J. H. Sherman, D. S. Luciano, *Human Physiology*, Mc Graw Hill, NY, 1994.

[17]. A. Algra, H. L. Brun, C. Zeelenberg," An algorithm for computer measurement of QT intervals in the 24 hour ECG," *Computers in Cardiology*, IEEE Computer Society Press, pp. 117-119, 1987.

[18]. J. G. Webster, *Medical Instrumentation: Application and Design*, Houghton Mifflin Company, MA, 1992.

[19]. A. V. D. Loo, W. Arendts, S. H. Hohnloser," Variablity of QT measurement techniques in the surface electrocardiogram in patients with acute myocardial infarction and in normal subjects," *American Journal of Cardiology*, vol. 74, pp. 1113-1118, 1994.

[20]. K. Hnatkova, M. Malik, J. Kautzner, Yi Gang, A. J. Camm," Adjustment of QT dispersion assessed from 12 lead electrocardiograms for different numbers of analyzed electrocardiographic leads: comparison of stability of different methods." *British Heart Journal, vol. 72*, pp. 390-396, 1994.

[21]. N. B. Maclaughlin, Ronald W. F. Campbell, A. Murray," Comparison of automatic QT measurement techniques in the normal 12 lead electrocardiogram," *British Heart Journal*, vol. 74, pp. 84-89, 1995.

[22]. M. Kirvala, A. Y. Hankala," QT dispersion and autonomic function in diabetic and non-diabetic patients with renal failure," *British Journal of Anaesthesia*, vol. 73, pp. 801-804, 1994.

[23]. P. Laguna, N. V. Thakor, P. Caminal, R Jane, H. R. Yoon," New algorithm for QT interval analysis in 24 hour Holter ECG: performance and applications," *Med. & Biol. & Comput.*, vol.28, pp. 67-73, 1990.

[24]. S. G. Priori, C. Napolitano, L. Diehl, P. J. Schwartz," Dispersion of the QT interval: a marker of therapeutic efficiency in the long QT syndrome," *Circulation*, vol. 89, pp. 1681-1689, 1994.

[25]. E. Lepeschkin, B. Surawicz," The measurement of the QT interval of the electrocardiogram," *Circulation*, vol. 6, pp. 378-388, 1952.

[26]. M. Alberti, M. Merri, J. Benhorin, E. Locati, A. J. Moss," Electrocardiographic precordial interlead variability in normal individuals and with long QT syndrome," *Computers in Cardiology*, IEEE Computer Society, pp. 475-478, 1991.

[27]. S. S. Lo, C. J. Mathias, M. S. Sutton," QT interval and dispersion in primary autonomic failure," *Heart*, vol. 75, pp. 498-501, 1996.